

***r*-mode instability of neutron stars in Low-mass X-ray binaries: effects of Fermi surface depletion and superfluidity of dense matter**

J. M. Dong^{1,2}

¹*Institute of Modern Physics, Chinese Academy of Sciences, Lanzhou 730000, China*

²*School of Physics, University of Chinese Academy of Sciences, Beijing 100049, China*

(Dated: January 19, 2021)

The nucleon-nucleon correlation between nucleons leads to the Fermi surface depletion measured by a Z -factor in momentum distribution of dense nuclear matter. The roles of the Fermi surface depletion effect (Z -factor effect) and its quenched neutron triplet superfluidity of nuclear matter in viscosity and hence in the gravitational-wave-driven r -mode instability of neutron stars (NSs) are investigated. The bulk viscosity is reduced by both the two effects, especially the superfluid effect at low temperatures which is also able to reduce the inferred core temperature of NSs. Intriguingly, due to the neutron superfluidity, the core temperature of the NSs in known low-mass X-ray binaries (LMXBs) are found to be clearly divided into two groups: high and low temperatures which correspond to NSs with short and long recurrence times for nuclear-powered bursts respectively. Yet, a large number of NSs in these LMXBs are still located in the r -mode instability region. If the density-dependent symmetry energy is stiff enough, the occurrence of direct Urca process reduces the inferred core temperature by about one order of magnitude. Accordingly, the contradiction between the predictions and observations is alleviated to some extent, but some NSs are still located inside the unstable region.

Key words: gravitational waves – stars: neutron – stars: oscillations

I. INTRODUCTION

A great deal of attention has been paid to gravitational waves following its discovery from binary black holes merge (Abbott et al. 2016) and binary neutron stars (NSs) merge (Abbott et al. 2017). As a species of compact objects, NSs themselves can radiate gravitational waves due to for example the magnetic deformation (Bonazzola & Gourgoulhon 1996; Regimbau & de Freitas Pacheco 2001; Stella et al. 2005; Dall’Osso, Shore & Stella 2009; Marassi et al. 2011, Cheng et al. 2015, 2017) and r -mode instability (Andersson 1998). The r mode is a class of fluid mode of oscillation with Coriolis force as restoring force which is analogous to Earth’s Rossby waves, leading to the emission of gravitational waves in hot and rapidly rotating NSs due to the Chandrasekhar-Friedmann-Schutz instability, and hence it prevents the pulsars (rotating NSs) from reaching their Kepler rotational frequency Ω_{Kepler} . The emission of gravitational waves is able to excite r modes in NS core in turn and causes the oscillation amplitude to grow, hence resulting in a positive feedback. Such gravitational radiation induced by the r -mode instability is perhaps detectable with ground-based instruments in the coming years, and thus potentially provides a probe to uncover the interior information of NSs. On the other hand, the temperature-dependent damping mechanisms attributed to the bulk and shear viscosities, hinder the growth of the r mode. The r -mode instability window borders a critical curve that is determined by the balance of evolution time scales (r -mode driving and viscosity damping time scales are equal) in the frequency-temperature ($\nu_s - T$) plane. Above this critical curve the r -mode instability is active. In other words, the unstable window depends on the competition between the gravitational radiation and the viscous dissipation (see e.g. Andersson & Kokkotas 2001, Haskell 2015, Kostas et al. 2016, for review).

The low mass X-ray binary (LMXB) is a binary system where a compact object such as a NS (We discuss this case in the present work) is accreting matter from its low-mass companion that fills its Roche lobe. Ho et al. (2011) assumed that the spin-up torque from accretion is balanced by the spin-down torque from gravitational radiation due to the unstable r -mode, and the associated heating is equal to cooling via neutrino emissions, and therefore concluded that many NSs are located in the

r -mode instability region. Since the r -mode instability limits the spin-up of accretion powered millisecond pulsars in LMXBs, the rapidly rotating pulsars, such as the PSR J1748-2446ad rotating at 716 Hz, are difficult to understand. A better understanding of relevant damping mechanisms is particularly necessary.

Bulk viscosity appears, if the perturbations in pressure and density induced by the r -mode oscillations drives the dense matter away from β -equilibrium. Consequently, energy is dissipated as the system tries to restore its chemical equilibrium because of weak interaction. The bulk viscosity due to the modified Urca reactions (or perhaps the direct Urca for large mass NSs) provides the dominant dissipation mechanism at high temperatures ($\gtrsim 10^9$ K). However, at low temperatures ($\lesssim 10^9$ K), the shear viscosity caused by the neutron scattering and electron scattering or crust-core interface, is the primary mechanism for the damping of r modes. The viscosity is expected to be affected significantly by the superfluidity.

Superfluidity is an intriguing feature of dense nuclear matter, which receives great interest since it plays an essential role in the NS thermal evolution (Yakovlev et al. 1999, 2001; Page et al. 2004, 2006). Dong et al. (2013, 2016) found that the neutron 3PF_2 superfluidity for pure neutron matter or β -stable nuclear matter is strongly reduced by about one order of magnitude by the Fermi surface depletion effect (i.e., Z -factor effect) with the help of the microscopic Brueckner theory starting from bare nucleon-nucleon interactions. The nucleon-nucleon correlation, in particular the short-range correlation including short-range repulsion and tensor interaction, is so strong that it creates a high-momentum tail, giving rise to the Z -factor. The Z -factor at the Fermi surface is equal to the discontinuity of the occupation number in momentum distribution according to the Migdal-Luttinger theorem (Migdal 1957), as shown in the inset of Fig. 1(a). Therefore, it characterizes the deviation from the right-angle momentum distribution of perfect degenerate Fermi gas at zero-temperature, and hinders the particle transitions around the Fermi surface which could affect many properties of fermion systems related to particle-hole excitations. For instance, the Z -factor has far-reaching impact on the nuclear structure (Subedi et al. 2008; Hen et al. 2014), superfluidity of dense nuclear matter (Dong et al. 2013, 2016), NS thermal evolution (Dong et al. 2016), and the European Muon Collaboration effect (Hen et al. 2017; Duer et al. 2018), highlighting its fundamental importance. In the present work, the influences of the Z -factor along with its quenched superfluidity on the r -mode instability of NSs in LMXBs are investigated in detail.

II. EFFECTS OF THE Z -FACTOR AND ITS QUENCHED SUPERFLUIDITY ON VISCOSITY

In addition to depressing the superfluidity, the Z -factor effect is also able to change the viscosity directly because of the particle number depletion at the Fermi surface. For the neutron and proton Z -factors at the Fermi surfaces of β -stable NS matter at different nucleon number density ρ , we use simple formulas that depend on several parameters to fit the results of Dong et al. (2016) which is achieved from the Brueckner theory using the Argonne V18 nucleon-nucleon interaction plus a microscopic three-body force, given by

$$\begin{aligned} Z_{F,n}(\rho) &= 0.907 - 0.233\rho - 0.480\rho^2 + 0.481\rho^3, \\ Z_{F,p}(\rho) &= \begin{cases} 0.351 + 2.332\rho, & \rho \leq 0.15 \text{ fm}^{-3} \\ 0.656 + 0.451\rho - 1.151\rho^2 + 0.576\rho^3, & \rho > 0.15 \text{ fm}^{-3} \end{cases} \end{aligned} \quad (1)$$

for the sake of application, where the fraction of each component for β -stable matter is determined by the well-known variational APR equation of state (EOS) (Akmal et al. 1998). The non-rotating NS maximum mass of $2.2M_\odot$, the canonical NS radius of 11.6 km, and stellar thermal evolution obtained from this APR EOS are compatible with astrophysical observations (Page et al. 2004), and it is one of the most popular EOS to be employed to study the NS interior physics. The isospin-dependent part of EOS, i.e., the symmetry energy, from the Brueckner-Hartree-Fock approach is so stiff that the direct Urca (DUrca) reaction occurs even in $1.2M_\odot$ low-mass NSs (Yin & Zuo 2013), which is not consistent with the current understanding that the DUrca process does not occur in $1.4M_\odot$ canonical NSs (Lattimer & Prakash 2004; Page et al. 2004; Brown et al. 2018). Fortunately, the Z -factor-quenched superfluidity is so weak that the energy gap is not so sensitive to the nucleon-nucleon interaction and single-particle potential any longer, which is beneficial to obtain reliable superfluid gaps. For example, the inclusion of three-body

force does not change the weak neutron 3PF_2 superfluidity gap very much (Dong et al. 2013). The Z_F itself of neutron-rich matter is not very sensitive to the isospin asymmetry β at densities of interest if $\beta > 0.5$ (Yin et al. 2013). Therefore, the inconsistent treatment here is not expected to change the final conclusions. Because the Fermi surface depletion hinders particle-hole excitation around the Fermi level, the bulk viscosity ξ , being related to neutrino emission, is expected to be reduced with the inclusion of the Z -factor. The momentum distribution function $n(k)$ of nucleons near the Fermi surface at finite temperature T (not quite high) is given by (Dong et al. 2016)

$$n(k) = \frac{Z_F}{1 + \exp\left(\frac{\omega - \mu}{T}\right)}, \quad k \approx k_F, \quad (2)$$

where ω is single-particle energy, and μ the chemical potential. The nucleon-nucleon correlation between nucleons quenches the occupation probability by a factor of Z_F at the Fermi surface.

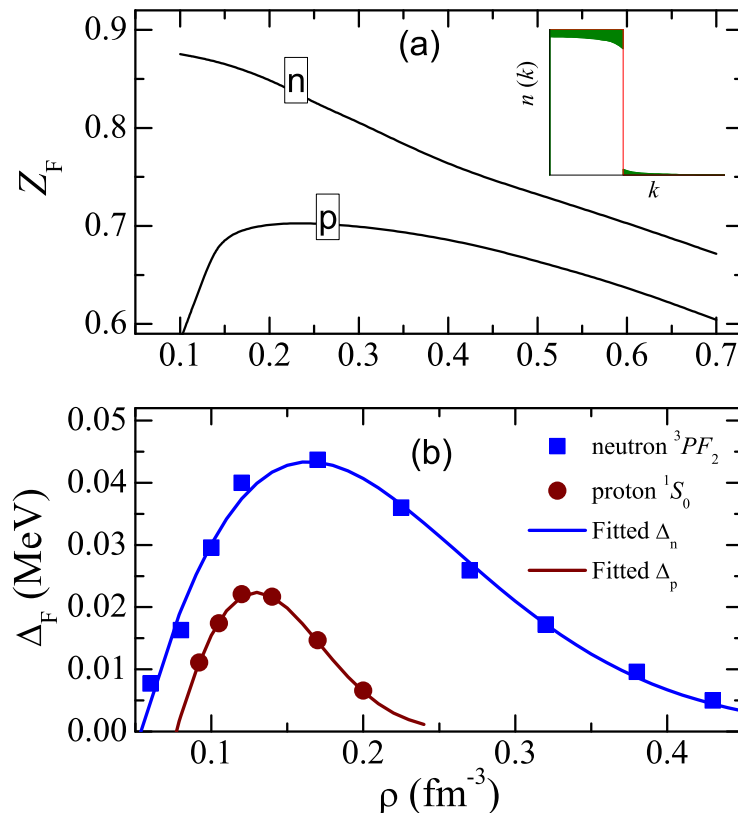


FIG. 1: (Color online) (a): Z -factor at the Fermi surface as a function of nucleon number density ρ in β -stable NS matter (Dong et al. 2016). The inset shows a schematic illustration of the momentum distribution due to the Z -factor effect. (b): neutron 3PF_2 superfluid gap VS. nucleonic density in β -stable matter (Dong et al. 2016; Li et al. 2020), compared with the fitting results that denoted by the solid curves.

The rapid cooling of the NS in Cas A has been revealed through the ten-year observations (Heinke & Ho 2010), which helps one to extract the interior information of NSs (Page et al. 2011; Shternin et al. 2011; Blaschke et al. 2012, 2013; Sedrakian 2013; Newton et al. 2013; Bonanno et al. 2014; Ho et al. 2015). Then combined with theoretical analysis, Page et al. (2011) claimed that this is the first direct evidence that neutron triplet superfluidity and proton singlet superconductivity occur at supranuclear densities within NSs, with the critical temperature for neutron 3P_2 superfluidity $T_{\text{cn,max}} = 5 \times 10^8$ K (the corresponding superfluid gap 0.08 MeV). However, Posselt et al. reported that a statistically significant temperature drop for the NS in Cas A is not present. Therefore, a reliable calculation of the superfluid gap theoretically is especially necessary. When the Z -factor effect is taken into account, the peak-value of neutron 3PF_2 superfluid gap is about 0.04 MeV for pure neutron matter as well as β -stable NS matter

(Dong et al., 2013, 2016), in agreement with other predictions (Ding et al. 2016) but much lower than the constrained value of 0.08 MeV by Page et al. (2011). The superfluid gap quenches all processes that involve elementary excitations around the Fermi surface, leading to remarkable effects on the neutrino emissivity, heat capacity, thermal conductivity, and hence NS thermal evolution. Since the core temperatures for NSs in LMXBs were inferred to be $(1 \sim 3) \times 10^8 \text{K}$ (Ho et al. 2011) which is basically below the critical temperature of neutron 3PF_2 superfluidity, such a superfluidity is expected to affect the r -mode instability distinctly.

For the angular-averaged neutron 3PF_2 superfluid gap and proton 1S_0 superconducting gap quenched by the Z -factor effect at zero-temperature in β -stable matter, we fit the results of Dong et al. (2016) and Dong (2019) obtained with the generalized Bardeen-Cooper-Schriffer method combined with the Brueckner theory, as summarized in Fig. 1 (b), which take the form of

$$\Delta_n(\rho) = (0.943\rho - 0.050) \exp\left[-\left(\frac{\rho}{0.177}\right)^{1.665}\right], \quad (3)$$

$$\Delta_p(\rho) = (1.015\rho - 0.078) \exp\left[-\left(\frac{\rho}{0.136}\right)^{2.823}\right], \quad (4)$$

as a function of nucleon number density ρ and the corresponding critical temperature is $T_c = 0.57\Delta$ (Page et al. 2004). The results perhaps are also useful to help one to understand pulsar glitches. The proton 1S_0 gap is much smaller than the neutron 3PF_2 gap, and its superfluid domain is rather narrow. In addition, the proton fraction is much smaller than the neutron one for β -stable NS matter. Therefore, the proton superconductivity will not be considered in the following discussion.

We explore the influence of the Z -factor and superfluidity on the viscosity. The bulk viscosity of $npe\mu$ matter is mainly determined by the reaction of DUrca process $n \rightarrow p + l + \bar{\nu}_l$, $p + l \rightarrow n + \nu_l$ together with the modified Urca (MUrca) processes $n + N \rightarrow p + N + l + \bar{\nu}_l$, $p + N + l \rightarrow n + N + \nu_l$, where N denotes neutron (n) or proton (p) and l denotes electron (e) or muon (μ). The DUrca process is most efficient for neutrino (ν) emission, but it occurs only if the proton fraction is high enough to reach a threshold. Frankfurt et al. (2008) concluded that the high-momentum tail of the nucleon momentum distribution induced by the short-range correlation leads to a significant enhancement of the neutrino emissivity of the DUrca process, and this rapid process can be opened even at low proton fraction. However, Dong et al. (2016) gave the opposite conclusions, that is, the neutrino emissivity is reduced instead of enhanced, and the threshold condition for the DUrca reaction is almost unchanged. The β -decay of neutrons and its inverse process can be cyclically driven just by thermal excitations, and high momentum tail cannot participate in the DUrca process and also the MUrca processes. The explicit discussion are presented in Dong et al. (2016).

The partial bulk viscosity of $npe\mu$ matter induced by a non-equilibrium DUrca process without the Z -factor effect ($Z = 1$) is written as (Haensel et al. 2000)

$$\xi_{l,0}^{(D)} = K \int_0^\infty dx_\nu x_\nu^2 \int dx_n dx_p dx_l \left\{ f(x_n) f(x_p) f(x_l) \cdot \left[\delta(x_n + x_p + x_l - x_\nu + \zeta) - \delta(x_n + x_p + x_l - x_\nu - \zeta) \right] \right\}, \quad (5)$$

through a complicated deduction, where $f(x) = 1/(1 + e^x)$ in the phase space integral is a Fermi-Dirac function and K is related to the temperature T , r -mode angular frequency ω , nuclear matter EOS and possible superfluid gap. ζ is a parameter to measure the deviation of the system from β -equilibrium. Due to the strong degeneracy of nucleons and electrons, the main contribution to the above integral comes from the very narrow regions of momentum space near the corresponding Fermi surfaces k_F , just as the calculation of neutrino emissivity of the DUrca process in Yakovlev et al. (2001). If the Z -factor effect is included, the above Fermi-Dirac distribution $f(x)$ near the Fermi surface for nucleons should be replaced by Eq. (2), i.e., $Z_F/(1 + e^x) = Z_F f(x)$, resulting in an additional factor $Z_{F,n} Z_{F,p}$ appearing in the right hand side of Eq. (5). Therefore, the bulk viscosity induced by DUrca reaction is given by

$$\xi_l^{(D)} = Z_{F,n} Z_{F,p} \xi_{l,0}^{(D)}. \quad (6)$$

The explicit expression of the $\xi_{l,0}^{(D)}$ takes the form of (Haensel et al. 2000)

$$\xi_{l,0}^{(D)} = 8.553 \times 10^{24} \frac{m_n^* m_p^*}{m_n m_p} \left(\frac{n_e}{0.16} \right)^{1/3} \cdot \frac{T_9^4}{\omega_4^2} \left(\frac{C_l}{100 \text{ MeV}} \right)^2 \Theta_{npl} \text{ g cm}^{-1} \text{ s}^{-1}, \quad (7)$$

with $\omega_4 = \omega/(10^4 \text{ s}^{-1})$, $T_9 = T/(10^9 \text{ K})$ and $C_l = 4(1 - 2Y_p)\rho dS(\rho)/d\rho - k_{F,l}^2/[12(1 - 2Y_p)S(\rho)]$ where Y_p and $S(\rho)$ are the proton fraction and density-dependent symmetry energy respectively. n_e and m^* are the electron number density in units of fm^{-3} and nucleonic effective mass, respectively. The step function is $\Theta_{npl} = 1$ if the DUrca process opens for $k_{F,n} < (k_{F,l} + k_{F,p})$. The $\xi_{l,0}^{(D)}$ could include the superfluid effect by a multiplying control function whose tedious expression can be consulted in Haensel et al. (2000). The angular frequency ω of the r -mode ($l = m = 2$) in a corotating frame is given by $\omega = 2m\Omega/l(l+1)$ (Andersson 2001), where Ω is the angular velocity of the rotating star. Similarly, the distribution function $f(x_n)f(x_p)f(x_N)f(x_{N'})$ that appears in phase space integral (Haensel et al. 2001) for the bulk viscosity produced by the MUrca processes, is replaced by $[Z_{F,n}f(x_n)][Z_{F,p}f(x_p)][Z_{F,N}f(x_N)][Z_{F,N'}f(x_{N'})]$, and thus we obtain

$$\xi_l^{(Mn)} = Z_{F,n}^3 Z_{F,p} \xi_{l,0}^{(Mn)}, \quad (8)$$

$$\xi_l^{(Mp)} = Z_{F,n} Z_{F,p}^3 \xi_{l,0}^{(Mp)}, \quad (9)$$

where the superscript $N = n(p)$ denotes the neutron (proton) branch of the MUrca processes. The $\xi_{l,0}^{(Mn)}$ and $\xi_{l,0}^{(Mp)}$ are given by (Haensel et al. 2001)

$$\xi_{e,0}^{(Mn)} = 1.49 \times 10^{19} \left(\frac{m_n^*}{m_n} \right)^3 \frac{m_p^*}{m_p} \left(\frac{n_p}{0.16} \right)^{1/3} \cdot \frac{T_9^6}{\omega_4^2} \left(\frac{C_e}{100 \text{ MeV}} \right)^2 \alpha_n \beta_n \text{ g cm}^{-1} \text{ s}^{-1}, \quad (10)$$

$$\xi_{e,0}^{(Mp)} = \xi_{e,0}^{(Mn)} \left(\frac{m_p^*}{m_n^*} \right)^2 \frac{(3k_{F,p} + k_{F,e} - k_{F,n})^2}{8k_{F,p}k_{F,e}} \Theta_{pe}, \quad (11)$$

$$\xi_{\mu,0}^{(Mn)} = \xi_{e,0}^{(Mn)} \left(\frac{k_{F,\mu}}{k_{F,e}} \right) \left(\frac{C_\mu}{C_e} \right)^2, \quad (12)$$

$$\xi_{\mu,0}^{(Mp)} = \xi_{e,0}^{(Mn)} \left(\frac{C_\mu m_p^*}{C_e m_n^*} \right)^2 \frac{(3k_{F,p} + k_{F,\mu} - k_{F,n})^2}{8k_{F,p}k_{F,e}} \Theta_{p\mu}, \quad (13)$$

with $\Theta_{pl} = 1$ for $k_{F,n} < (k_{F,l} + 3k_{F,p})$ and $\Theta_{pl} = 0$ otherwise. We use $\alpha_n = 1.76 - 0.63(1.68 \text{ fm}^{-1}/k_{F,n})^2$, $\beta_n = 0.68$ from Page et al. (2004) here. The tedious control functions to measure the superfluid effect can be seen in Haensel et al. (2001).

The calculated ξ involving electron and muon branches as a function of the temperature T , without and with the Z-factor and its quenched superfluidity, are displayed in Fig. 2, taking the density $\rho = 0.17 \text{ fm}^{-3}$ and rotation angular frequency $\Omega = 10^4 \text{ s}^{-1}$ as an example. The Z-factor reduces the ξ by about 50% at $\rho = 0.17 \text{ fm}^{-3}$, and such a Z-factor effect can be more substantial at high densities, according to Eqs. (1,8,9). When the temperature drops below the neutron ${}^3\text{PF}_2$ superfluid critical temperature, the ξ is significantly reduced. For instance, at the temperature $T = 10^7 \text{ K}$, the ξ is lowered by about six orders of magnitude. The corresponding damping time scale τ_ξ is thus enlarged especially at low temperatures. However, the bulk viscosity dominates the damping mechanism just at high temperatures ($\gtrsim 10^9 \text{ K}$), at which the neutron ${}^3\text{PF}_2$ superfluidity vanishes. It has been concluded that shear viscosity primarily stems from electron scattering instead of neutron scattering (Shternin & Yakovlev 2008; Vidana 2012) at temperatures $T \gtrsim 10^7 \text{ K}$. Shang et al. found that the neutron shear viscosity η_n is enhanced by the Z-factor effect but is lowered much more strongly by the onset of neutron triplet superfluidity. As a result, the electron shear viscosity η_e is generally larger than the neutron one η_n even at very low temperatures. So we still employ the widely-used formulas for electron shear viscosity η_e (Shternin & Yakovlev 2008; Alford et al. 2012) and unimportant neutron shear viscosity η_n (Cutler & L. Lindblom

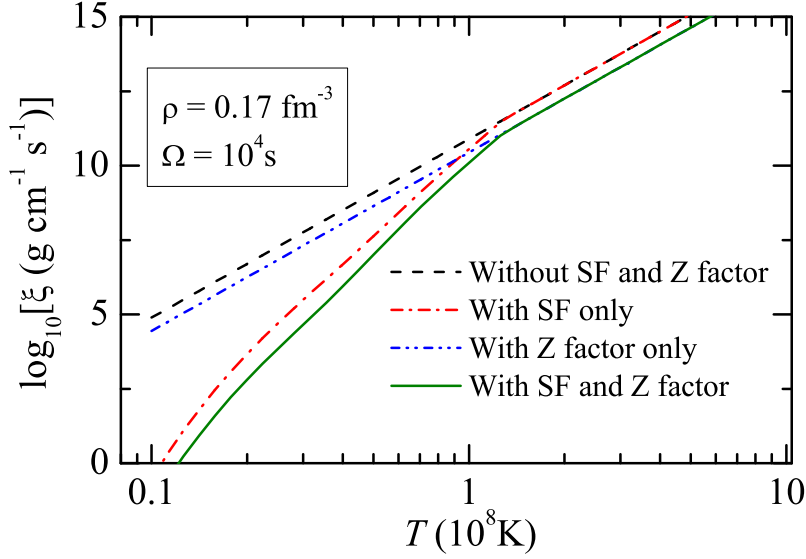


FIG. 2: (Color online) The logarithmic ξ ($\text{g cm}^{-1}\text{s}^{-1}$) under different temperature T (in units of 10^8 K). The angular frequency is $\Omega = 10^4$ s^{-1} . The calculated results without the superfluidity (SF) and Z-factor, with Z-factor only, with the 3P_F_2 superfluidity only, and with both the superfluidity and Z-factor, are shown for comparison.

1987) which are respectively given by

$$\eta_e = 4 \times 10^{-26} (Y_p n_b)^{14/9} T^{-5/3} \text{ g cm}^{-1}\text{s}^{-1}, \quad (14)$$

$$\eta_n = 2 \times 10^{18} \rho_{15}^{9/4} T_9^{-2} \text{ g cm}^{-1}\text{s}^{-1}, \quad (15)$$

where ρ_{15} and T_9 are the density and temperature in units of $10^{15} \text{ g cm}^{-3}$ and 10^9 K, respectively. n_b is baryon number density in units of cm^{-3} here.

The time scales for bulk viscosity (Lindblom et al. 2002; Nayyar et al. 2006), shear viscosity (Lindblom et al. 1998), and a r -mode growth due to the gravitation radiation (Lindblom et al. 1998) are respectively given by

$$\frac{1}{\tau_\xi} = \frac{4\pi}{690} \left(\frac{\Omega^2}{\pi G \bar{\rho}} \right)^2 R^{2l-2} \left(\int_0^R \rho r^{2l+2} dr \right)^{-1} \int_0^R \xi \left(\frac{r}{R} \right)^6 \left[1 + 0.86 \left(\frac{r}{R} \right)^2 \right] r^2 dr, \quad (16)$$

$$\frac{1}{\tau_\eta} = (l-1)(2l+1) \left(\int_0^R \rho r^{2l+2} dr \right)^{-1} \int_0^R \eta r^{2l} dr, \quad (17)$$

$$\frac{1}{\tau_{\text{GW}}} = \frac{32\pi G \Omega^{2l+2}}{c^{2l+3}} \frac{(l-1)^{2l}}{[(2l+1)!!]^2} \left(\frac{l+2}{l+1} \right)^{2l+2} \left(\int_0^R \rho r^{2l+2} dr \right), \quad (18)$$

where $\bar{\rho}$ is the average density and G is the gravitational constant. The viscous dissipation at the viscous boundary layer (VBL) of perfectly rigid crust and fluid core is proposed as the primary damping mechanism in some literatures, and its time scale is (Bildsten & Ushomirsky 2000; Lindblom et al. 2000)

$$\tau_{\text{VBL}} = \frac{1}{2\Omega} \frac{2^{l+3/2}(l+1)!}{l(2l+1)!!I_l} \sqrt{\frac{2\Omega R_c^2 \rho_c}{\eta_c}} \int_0^{R_c} \frac{\rho}{\rho_c} \left(\frac{r}{R_c} \right)^{2l+2} \frac{dr}{R_c}, \quad (19)$$

where ρ_c , R_c , and η_c are the density, radius and the shear viscosity of the NS matter at the outer edge of the core (or equivalently inner edge of the crust). In the case of $l = m = 2$ mode, the I_2 is 0.80411 (Lindblom et al. 2000; Rieutord 2001). Yet, a rigid crust is an ideal model. The relative motion (slippage) between the crust and core reduces the damping by as much as a factor of $f = 10^2 - 10^3$ (Levin & Ushomirsky 2001). In the present work, we select $f = 10^2$ as in the references of Ho et al.

(2011) with a slippage factor $\mathcal{S} = 0.1$. Such a role is questioned if the core-crust boundary is defined by a continuous transition from non-uniform matter to uniform matter through ‘nuclear pasta’ phases with different shapes (Pethick & Potekhin 1998), and consequently the VBL is smeared out (Gearheart et al. 2011).

An overall time scale of the r -mode, which includes the exponential growth induced by the Chandrasekhar-Friedmann-Schutz mechanism and the decay due to viscous damping, is given by $1/\tau = -1/\tau_{\text{GW}} + 1/\tau_{\xi} + 1/\tau_{\eta} + 1/f\tau_{\text{VBL}}$. If $1/\tau > 0$, the mode will exponentially grow, while it will quickly decay if $1/\tau < 0$. Therefore, a NS will be stable against the r -mode instability if its angular velocity Ω is smaller than a critical value Ω_c . A star with $\Omega > \Omega_c$ will lose its angular momentum through gravitational radiation until the Ω falls below the Ω_c .

III. EFFECTS OF THE Z-FACTOR AND THE SUPERFLUIDITY ON r -MODE INSTABILITY

Usually the stellar surface temperature can be obtained from the fitting of black-body spectra of LMXBs in quiescence, whereas the core temperature cannot be obtained readily. Ho et al. (2012) assumed that the stellar interior is isothermal and the heating is balanced by neutrino cooling in steady state NSs of LMXBs, i.e., $L_{\text{heat}} = L_{\nu}$, to infer the stellar core temperature for a NS with spin frequency $\nu_s = \Omega/2\pi$. The L_{heat} is given by $L_{\text{heat}} = 0.065(\nu_s/300\text{Hz})L_{\text{acc}}$ (Brown & Ushomirsky 2000), where L_{acc} is the accretion luminosity computed by using the observed flux and distance. Usually, one assumes a canonical NS cools via the MUrca processes when the core temperature $T \gtrsim 10^8$ K. Such a neutrino emission process can be depressed by the neutron ${}^3\text{PF}_2$ superfluidity substantially when the core temperature is below the critical temperature T_c . On the other hand, the superfluidity is able to enhance the emission due to the Cooper pair breaking and formation (PBF) process when the temperature is slightly below T_c . This PBF process tends to be more effective than the MUrca process, which could result in a rapid NS cooling (Page et al. 2011; Shternin et al. 2011).

We calculate the neutrino emissivity Q for $1.4M_{\odot}$ canonical NSs with the inclusion of the Z -factor and neutron superfluid effects. The neutrino emissivity for DUrca, MUrca and PBF processes are given as $Q^{(D)} = Z_{F,n}Z_{F,p}Q_0^{(D)}$, $Q^{(Mn)} = Z_{F,n}^3Z_{F,p}Q_0^{(Mn)}$, $Q^{(Mp)} = Z_{F,n}Z_{F,p}^3Q_0^{(Mp)}$ and $Q^{(PBF)} = Z_{F,n}^2Q_0^{(PBF)}$ (Dong et al. 2016). Here $Q_0^{(D)}$, $Q_0^{(Mn)}$, $Q_0^{(Mp)}$ and $Q_0^{(PBF)}$ are well-established emissivity that include the possible superfluid effect with control functions (see Yakovlev et al. 1999, 2001 for details) but without the Z -factor effect ($Z = 1$). The corresponding luminosity is calculated by volume integral $L = \int QdV$. The NS interior is assumed to be composed of $npe\mu$ dense matter without exotic degrees of freedom. The stellar structure for a nonrotating NS is established by integrating the Tolman-Oppenheimer-Volkov (TOV) equation with the EOS from the user-friendly IMP1 Skyrme energy density functional (Dong & Shang 2020). Such an EOS is close to the APR EOS because the APR EOS for pure neutron matter has been served as a calibration for building up the IMP1 Skyrme interaction (Dong & Shang 2020), and provides good description of neutron star properties. Within this EOS, the results do not depend substantially on the assumed stellar mass.

The calculated luminosity L_{MUrca} , L_{PBF} and the total neutrino luminosity $L_{\nu} = L_{\text{MUrca}} + L_{\text{PBF}}$ are presented in Fig. 3. At temperatures lower than the superfluid critical temperature T_c , L_{PBF} is about 2 ~ 3 orders of magnitude larger than the L_{MUrca} , resulting in a lower inferred core temperature T . The observed flux, distance and spin frequency from Watts et al. (2008) are applied to achieve the L_{heat} for NSs in known LMXBs. The intersection of the curve L_{ν} and L_{heat} gives the stellar core temperature for each NS. Unlike in Ho et al. (2011a, 2011b), each NS we discussed here has a unique inferred core temperature, and it lies in the range of $(1 \sim 3) \times 10^8$ K.

Figure 4 exhibits the $\nu_s - T$ plot where core temperatures T are inferred from $L_{\nu} = L_{\text{heat}}$ and spin frequency ν_s have been observed for NSs in these LMXBs. The error bar on the inferred T is not included here because it does not affect the following discussions. The r -mode instability window is determined by the time scale balance $1/\tau_{\text{GW}} = 1/\tau_{\xi} + 1/\tau_{\eta} + 1/f\tau_{\text{VBL}}$. This critical curve is almost not influenced by the Z -factor and superfluid effects because the electron shear viscosity contributes mainly to the viscous damping in this temperature range. When the Z -factor and superfluidity are excluded, most of these millisecond pulsars are located in the instability window, as shown in Fig. 4(a). When these two effects are included, the referred core temperature of some rapidly rotating NSs are reduced by a factor of around 2, as displayed in Fig. 4(b), being attributed to an enhanced

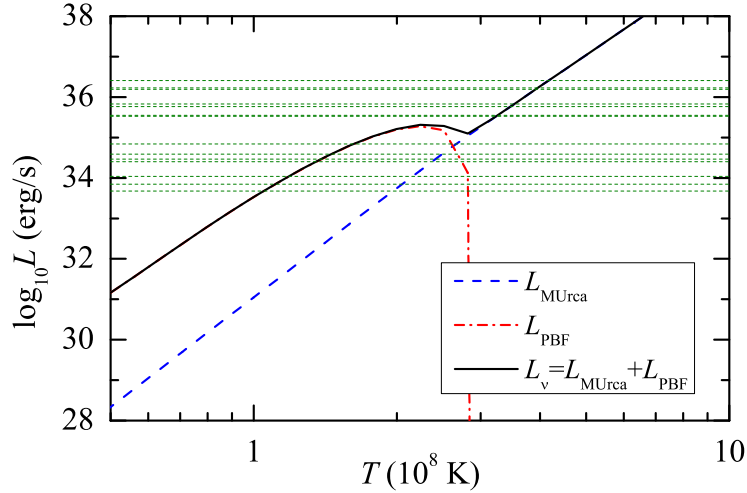


FIG. 3: (Color online) The calculated neutrino luminosity from the MUrcA, PBF processes for canonical NSs, where the Z -factor effect and its quenched neutron 3PF_2 superfluidity are included. The stellar structure is constructed based on the EOS from the IMP1 Skyrme interaction. The dashed horizontal lines denote the obtained L_{heat} for NSs in known LMXBs using the observed flux, distance and spin frequency (Watts et al. 2008). The intersection of the $L_{\text{heat}} = L_{\nu}$ yields the stellar core temperature for each NS.

neutrino emissivity from PBF process (the Z -factor itself does not contribute distinctly). Nevertheless, it is not evident to modify the conclusion that lots of systems locate inside the unstable region, even if the damping due to the VBL is included. So far, it is not fully understood what causes LMXBs to undergo long versus short recurrence time bursts. Intriguingly, as shown in Fig. 4(b), these NSs are clearly divided into two categories: high-temperature branch ($\sim 3 \times 10^8$ K) and low-temperature branch ($\sim 10^8$ K). The short LMXBs perhaps have high core temperature ($\sim 3 \times 10^8$ K) than long LMXBs ($\sim 10^8$ K), as proposed by Ho et al. (2011). A higher surface temperature is able to shorten the time intervals between ignition of nuclear burning.

The EOS used above is calculated by employing the IMP1 Skyrme force. The symmetry energy are not stiff sufficiently to allow the onset of the DUrcA processes for canonical NSs and even large mass NSs. Yet, recently Brown et al. (2018) showed that the NS in the transient system MXB1659-29 has a core neutrino luminosity that is consistent with the DUrcA reaction occurring in a small fraction of the core, substantially exceeds the MUrcA processes, and they fitted the NS mass $M \sim 1.6M_{\odot}$ in their model. We investigate the role of the symmetry energy in the $\nu_s - T$ relation, and employ the density-dependent symmetry energy written as

$$S(\rho) = 13.0 \left(\frac{\rho}{\rho_0} \right)^{2/3} + C_1 \left(\frac{\rho}{\rho_0} \right) + C_2 \left(\frac{\rho}{\rho_0} \right)^{\gamma}, \quad (20)$$

$$C_1 = 19.4 - \frac{18.3}{2.06 - 3\gamma \cdot 0.69^{\gamma}},$$

$$C_2 = 19.4 - C_1,$$

to supplement to the EOS of symmetric matter from IMP1 manually. It can be considered as an extension of the DDM3Y-shape expression (Mukhopadhyay et al. 2007; Dong et al. 2012; Dong et al. 2013; Fan et al. 2014) and enables us to reproduce the symmetry energy $S = 32.4$ MeV at nuclear saturation density ρ_0 and the slope parameter $L = 42$ MeV at $\rho = 0.11 \text{ fm}^{-3}$ (Dong et al. 2018). The only one free parameter γ or equivalently the slope parameter L (distinguished from aforementioned luminosity L) at ρ_0 controls its density-dependence (i.e., whether the symmetry energy is stiff or soft). Vidana (2012) and Wen et al. (2012) discussed the effects of symmetry energy on the r -mode instability, which give opposite conclusions. Figure 5 presents the calculated r -mode instability critical curve and the location of each NS with $M_{\text{TOV}} = 1.6M_{\odot}$ in LMXBs in the $\nu_s - T$ plot, taking $L = 50, 60$ and 80 MeV as examples. If the DUrcA process opens, such as the $L = 60$ MeV case, the inferred core T is reduced

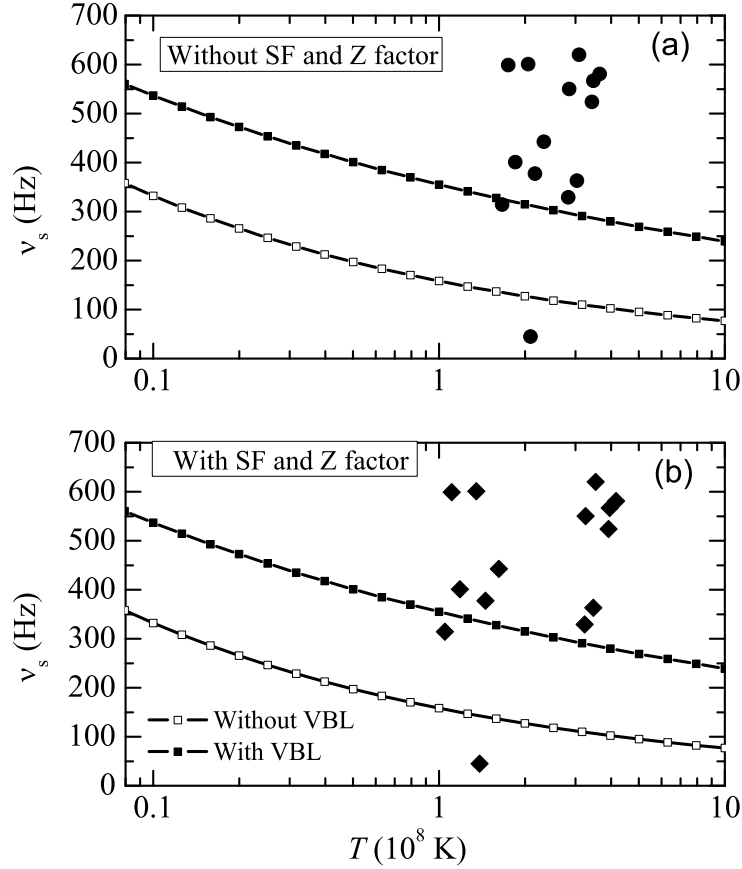


FIG. 4: The observed spin frequency ν_s and the inferred core temperature T for NSs in known LMXBs. The hallow squares do not include the VBL damping, namely $1/\tau_{\text{GW}} = 1/\tau_\xi + 1/\tau_\eta$. The black squares include the VBL damping, namely $1/\tau_{\text{GW}} = 1/\tau_\xi + 1/\tau_\eta + 1/f\tau_{\text{VBL}}$, with $f = 100$. Above the critical curves are the r -mode instability region for $M = 1.4M_\odot$ canonical NSs without (a) and with (b) the Z-factor and its quenched superfluidity (SF).

by about one order of magnitude because of the high efficiency of the DURca reaction. Although the neutrino emissivity of the DURca reaction can be about eight orders of magnitude larger than that of the MURca process, its influence on the inferred core temperature is only about one order of magnitude because of the strong temperature scaling in the $L_\nu - T$ relation. Many NSs are inside the stable region, and others are also located in but closer to the stability window. Therefore, the presence of the DURca process could alleviate the disagreement between the observed and the predicted results to a large extent. Yet, if the VBL is smeared out because of the nuclear pasta phases, the DURca process still cannot modify the conclusion that most NSs locate well inside the unstable region.

Additional damping mechanisms or physics perhaps is required to reconcile the theory and observations. The mutual friction due to vortices in a rotating superfluid (electrons scattered off of magnetized vortices) is claimed to be unlikely to suppress the r -mode instability in rapidly spinning NSs, but for a large ‘drag’ parameter \mathcal{R} the mutual friction is sufficiently strong to suppress this instability completely as soon as the core becomes superfluid (Haskell et al. 2009). Anyway, this vortex-mediated mutual friction damping is a rather complicated mechanism that is difficult to calculate precisely, calling for further investigation. In addition, the hyperonic bulk viscosity caused by nonleptonic weak interactions is also found to stabilize the oscillation mode effectively (Jha et al. 2010). Gusakov et al. (2014) argued that finite temperature effects in the superfluid core leads to a resonance coupling and enhanced damping of oscillation modes at certain temperatures, and therefore the rapidly rotating NSs may spend a long time at these resonance temperatures. Moreover, the theoretical understanding can be consistent with observations if the r -

mode saturation amplitude is so small that the gravitational wave torque cannot counteract the accretion torque although r -mode heating is balanced by stellar cooling. As a result, the r -mode instability has no impact on the spin or thermal evolution of NSs. The recent investigations indeed present low saturation amplitudes α_m . For instance, Haskell & Patruno (2017) constrained the amplitude of an unstable r -mode from the spinning down of PSR J1023+0038, and gave $\alpha_m \approx 5 \times 10^{-8}$. Haskell et al. (2012) concluded that for most known LMXBs in the unstable region one has $\alpha_m = 10^{-9} \sim 10^{-8}$. Using known X-ray upper bounds on the temperatures and luminosities of several non-accreting millisecond radio pulsars, Schwenzer et al. (2017) derived the r -mode amplitude as low as $\alpha_m \lesssim 10^{-8}$.

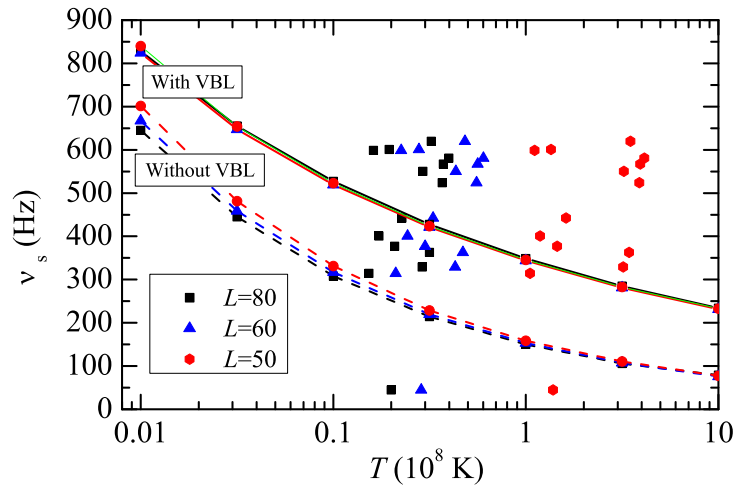


FIG. 5: (Color online) Similar to Fig. 4, but the NS masses are assumed to be $M_{\text{TOV}} = 1.6M_{\odot}$. The EOS with various density-dependent symmetry energy are employed, where the onset of the DUrca process due to a stiff symmetry energy could lead to a lower core temperature. The dashed (solid) curves are the critical curves without (with) the VBL damping, and $f = 10^2$.

IV. SUMMARY

We have investigated the bulk viscosity ξ and r -mode instability under the influence of both the Z -factor and its quenched neutron superfluidity, where the recently calculated superfluid gaps and Z -factors at Fermi surfaces within a microscopic nuclear many-body approaches are employed. The Z -factor effect reduces the bulk viscosity ξ by several times at most, while the neutron 3PF_2 superfluidity is able to reduce the ξ by several orders of magnitude when the core temperature T is lower than the critical temperature. With the inclusion of superfluidity, the PBF process opens when the stellar core temperature is slightly lower than the critical temperature, leading to an enhanced neutrino emission. As a result, the superfluidity decreases the inferred core temperature for some relatively low temperature NSs in LMXBs obviously. Interestingly, because of the neutron 3PF_2 superfluidity, the core temperature of the NSs in these discussed LMXBs are divided into two groups-high and low temperatures. These NSs with long recurrence times for nuclear-powered bursts are considered to have lower core temperature (10^8 K), while these with short recurrence times have high core temperatures (3×10^8 K). However, most NSs are still predicted to be r -mode instable. In other words, the introducing of the Z -factor and neutron triplet superfluidity cannot solve this problem fundamentally. If the DUrca process occurs due to a sufficiently stiff symmetry energy, the inferred core temperature is reduced by about one order of magnitude, many NSs are located in the r -mode stable window and others are closer to this region if the VBL damping is taken into account. In other words, more NSs will be inside the r -mode stability window for interactions which give larger values of symmetry energy slope L . However, the existence of most rapidly rotating NSs, such as the 716 Hz PSR J1748-2446 ad, remains a puzzle. If the r -mode saturation amplitude is too small to impact on the spin or thermal evolution of NSs, such as the

inferred $\alpha \approx 5 \times 10^{-8}$ from the spinning down of PSR J1023+0038 by Haskell & Patruno (2017), the theoretical understanding can be consistent with observations.

Acknowledgement

J. M. Dong would like to thank L. J. Wang for helpful suggestions. This work was supported by the National Natural Science Foundation of China under Grant No. 11775276, by the Strategic Priority Research Program of Chinese Academy of Sciences under Grant No. XDB34000000, by the Youth Innovation Promotion Association of Chinese Academy of Sciences under Grant No. Y201871.

Data Availability

The data used to support the findings of this study are available from the corresponding author upon request.

-
- Akmal A., Pandharipande V. R., Ravenhall D. G. 1998, Phys. Rev. C, 58, 1804
 Alford M. G., Mahmoodifar S., Schwenzer K., 2012, Phys. Rev. D, 85, 024007
 Andersson N., 2001, Class. Quant. Grav., 20, R105
 Andersson N., Kokkotas K. D., 2001, IJMPD, 10, 381
 Abbott B. P. et al., 2016, Phys. Rev. Lett, 116, 061102
 Abbott B. P. et al., 2017, Phys. Rev. Lett, 119, 161101
 Blaschke D., Grigorian H., Voskresensky D. N., Weber F. 2012, Phys. Rev. C, 85, 022802(R)
 Blaschke D., Grigorian H., Voskresensky D. N. 2013, Phys. Rev. C, 88, 065805
 Bildsten L., Ushomirsky G., 2000, ApJ, 529, L33
 Bonanno A., Baldo M., Burgio G. F., Urpin V. 2014, A&A, 561, L5
 Bonazzola S., Gourgoulhon E., 1996, A&A, 312, 675
 Brown, E. F., Cumming, A., Fattoyev, F. J., Horowitz, C. J., Page, D., Reddy, S., 2018, Phys. Rev. Lett., 120, 182701
 Brown E. F., Ushomirsky G., 2000, ApJ, 536, 915
 Cheng Q., Yu Y. W., Zheng X. P., 2015, MNRAS 454, 2299
 Cheng Q., Zhang S. N., Zheng X. P., 2017, Phys. Rev. D, 95, 083003
 Cutler C., Lindblom L., 1987, ApJ, 314, 234
 Dall’Osso S., Shore S. N., Stella L., 2009, MNRAS, 398, 1869
 Ding D., Rios A., Dussan H., Dickhoff W. H., Witte S. J., Carbone A., Polls A., 2016, Phys. Rev. C, 94, 025802
 Dong J., Zhang H., Wang L., Zuo W., 2013, Phys. Rev. C, 88, 014302
 Dong J. M., Lombardo U., Zhang H. F., Zuo W., 2016, ApJ, 817, 6
 Dong J., Zuo W., Gu J., Lombardo U., 2012, Phys. Rev. C, 85, 034308
 Dong J. M., 2019, Pairing and neutron star cooling, private communication
 Dong J. M., Lombardo U., Zuo W., 2013, Phys. Rev. C, 87, 062801(R)
 Dong J. M., Shang X. L., 2020, Phys. Rev. C, 101, 014305
 Dong J. M., Wang L. J., Zuo W., Gu J. Z., 2018, Phys. Rev. C, 97, 034318
 Duer M. *et al.*, 2018, Nature, 560, 617
 Fan X., Dong J., Zuo W., 2014, Phys. Rev. C, 89, 017305
 Frankfurt L., Sargsian M., Strikman M., 2008, IJMPA, 23, 2991
 Gearheart M., Newton W. G., Hooker J., Li B., 2011, MNRAS, 418, 2343
 Gusakov M. E., Chugunov A. I., Kantor E. M., 2014, Phys. Rev. Lett., 112, 151101
 Haensel P., Levenfish K. P., Yakovlev D. G., 2000, A&A, 357, 1157

Haensel P., Levenfish K. P., Yakovlev D. G., 2001, *A&A*, 372, 130
Haskell B., 2015, *IJMPE*, 24, 1541007
Haskell B., Andersson N., Passamonti A., 2009, *MNRAS*, 397, 1464
Haskell B., Degenaar N., Ho W. C. G., 2012, *MNRAS*, 424, 93
Haskell B., Patruno A., 2017, *Phys. Rev. Lett.*, 119, 161103
Heinke C. O., Ho W. C. G., 2010, *ApJL*, 719, L167
Hen O. *et al.*, 2014, *Science*, 346, 614
Hen O., Miller G. A., Piasezky E., Weinstein L. B., 2017, *Rev. Mod. Phys.*, 89, 045002
Hessels J. W. T. *et al.*, 2006, *Science*, 311, 1901
Ho W. C. G., 2011, *MNRAS*, 418, L99
Ho W. C. G., Andersson N., Haskell B., 2011, *Phys. Rev. Lett.*, 107, 101101
Ho W. C. G., Elshamouty K. G., Heinke C. O., Potekhin A. Y., 2015, *Phys. Rev. C*, 91, 015806
Jha T. K., Mishra H., Sreekanth V., 2010, *Phys. Rev. C*, 82, 025803
Kadanoff L. P., Baym G., 1962, *Quantum Statistical Mechanics*, (New York)
Kokkotas K. D., Schwenzera K., 2016, *Eur. Phys. J. A*, 52, 38
Lattimer J. M., Prakash M., 2004, *Science*, 304, 536
Levin Y., Ushomirsky G., 2001, *MNRAS*, 324, 917
Lindblom L., Owen B. J., Ushomirsky G., 2000, *Phys. Rev. D*, 62, 084030
Lindblom L., Owen B. J., 2002, *Phys. Rev. D*, 65, 063006
Lindblom L., Owen B. J., Morsink S. M., 1998, *Phys. Rev. Lett.*, 80, 4843
Luttinger J. M., 1960, *Phys. Rev.*, 119, 1153
Marassi S., Ciolfi R., Schneider R., Stella L., Ferrari V., 2011, *MNRAS*, 411, 2549
Migdal A. B., 1957, *Sov. Phys. JETP*, 5, 333
Mukhopadhyay T., Basu D. N., 2007, *Nucl. Phys. A*, 789, 201
Nayyar M., Owen B. J., 2006, *Phys. Rev. D*, 73, 084001
Newton W. G., Murphy K., Hooker J., Li B.-A., 2013, *ApJL*, 779, L4
Page D., Lattimer J. M., Prakash M., Steiner A. W., 2004, *ApJS*, 155, 623
Page D., Geppert U., Weber F., 2006, *Nucl. Phys. A*, 777, 497
Page D., Prakash M., Lattimer J. M., Steiner A. W., 2011, *Phys. Rev. Lett.*, 106, 081101
Pethick C., Potekhin A. Y., 1998, *Phys. Lett. B*, 427, 7
Posselt B., Pavlov G. G., Suleimanov V., Kargaltsev O., 2013, *ApJ*, 779, 186
Regimbau T., de Freitas Pacheco J. A., 2001, *A&A*, 374, 182
Rieutord M., 2001, *ApJ*, 550, 443
Schwenzer K., Boztepe T., Güver T., Vurgun E., 2017, *MNRAS*, 466, 2560
Sedrakian A., 2013, *A&A*, 555, L10
Shang X. L., *et al.*, (unpublished)
Shternin P. S. *et al.*, 2011, *MNRAS*, 412, L108
Shternin P. S., Yakovlev D. G., 2008, *Phys. Rev. D*, 78, 063006
Subedi R. *et al.*, 2008, *Science*, 320, 1476
Vidana I., 2012, *Phys. Rev. C*, 85, 045808
Watts A. L., Krishnan B., Bildsten L., Schutz B. F., 2008, *MNRAS*, 389, 839
Wen D. -H., Newton W. G., Li B.-A., 2012, *Phys. Rev. C*, 85, 025801
Yakovlev D. G., Levenfish K. P., Shibano Y. A., 1999, *Phys. Uspekhi*, 42, 737
Yakovlev D. G., Kaminker A. D., Gnedin O. Y., Haensel P., 2001, *Phys. Rep.*, 354, 1
Yin P., Li J. Y., Wang P., Zuo W., 2013, *Phys. Rev. C*, 87, 014314
Yin P., Zuo W., 2013, *Phys. Rev. C*, 88, 015804